

Statistical evaluation of clusters derived by nonlinear mapping of EEG spatial patterns

John M. Barrie ^{a,c,*}, David Holcman ^b, Walter J. Freeman ^c

^a Department of Biophysics, Neurobiology Division, University of California at Berkeley, Berkeley, CA 94720-3200, USA

^b Department of Mathematics, Paris VI University, 4 Place Jussieu, Paris 75005, France

^c Department of Molecular and Cell Biology, Neurobiology Division, 129 Life Science Addition, University of California at Berkeley, Berkeley, CA 94720-3200, USA

Received 10 September 1998; received in revised form 23 March 1999; accepted 25 March 1999

Abstract

New methods were devised to improve the discrimination of EEG spatial amplitude patterns recorded from arrays of 64 electrodes placed on visual, auditory or somatic cortex. The 64 traces shared a spatially coherent, aperiodic carrier wave with a spatial pattern of amplitude modulation (AM). Previous observations on AM patterns from rabbits trained to discriminate conditioned stimuli with reinforcement (CS +) and without (CS –) had revealed epochs between the CS and the CR in which AM patterns on CS + trials could be distinguished from AM patterns on CS – trials. The AM patterns were expressed by points in 64-space that formed clusters. Levels of CS –/CS + pattern separation were quantified by a pair-wise Euclidean distance method with cross-validation. The present study documents use of the technique for nonlinear mapping (NLM) to project the 64-dimensional structure onto a plane while preserving the relative distances between all points. The goodness of classification by the Euclidean distance measure was the same or improved after projection. Whereas the Euclidean distance measure only gave pair-wise classifications, the planar displays showed the patterns for multiple clusters simultaneously. These NLM-based methods revealed previously unrecognized structures within distributions of AM patterns in sensory cortices in the time period between the CS and CR. © 1999 Elsevier Science B.V. All rights reserved.

Keywords: Auditory; Cluster analysis; Discriminative analysis; Neocortex; Rabbit; Somesthetic; Visual

1. Introduction

Recent advances in techniques for brain imaging have brought with them the need for better methods for measurement and classification of spatial patterns of neural activity. This requirement holds across the board for multichannel EEG, unit, optical, MRI, MEG, and PET recordings. The first step is visual inspection and comparisons of spatial patterns in two dimensions. Typically, no two patterns are identical, so the next step is to search for quantitative assays of differences between patterns and of their statistical significance. These assays require that spatial patterns be digitized in time and at pixels or channels in space. The resulting enormous data sets must be searched for recurring

patterns (Lilly and Cherry, 1954; DeMott, 1970; Freeman, 1975). The third step in managing high-dimensional data sets is to compress hundreds of spatial frames taken over time into two dimensions for visual display and statistical evaluation.

If one knows a priori the number of classes the patterns will fall into, one can compute averages over sets of spatial patterns to represent the classes taken sequentially, which is time ensemble averaging. If one knows also that the spatial differences are localized to particular parts of the frames, one can also compute the spatial patterns of the standard deviations and from these can calculate maps of *t* values, provided that the distributions of measurements over time at pixels or channels are shown to be normal. However, this method fails if the number of classes is not known in advance, and if the differences between patterns are not localized to one or a few channels or pixels in a set of

* Corresponding author. Tel.: +1-510-643-8896/642-4220; fax: +1-510-643-6791.

E-mail address: barriej@socrates.berkeley.edu (J.M. Barrie)

spatial patterns. Then all of the available data must be displayed without the use of time ensemble averaging.

A simplification of this problem was achieved in previous studies involving 64-channel EEG recordings from the visual, auditory, and somatic cortices of NZW rabbits trained to discriminate conditioned stimuli with reinforcement (CS+) and without it (CS−) (Freeman and Viana Di Prisco, 1986; Barrie et al., 1996). Visual displays of the 64 traces revealed a common wave form over the areas of cortex covered by the array on the order of 6×6 mm, which differed in phase and amplitude. The phase differences were under a quarter cycle of the dominant frequency of oscillation and were not related to behavior, so they were secondary in importance. The amplitude modulation of the carrier constituted a spatial AM pattern that was clearly related to behavior, because it changed consistently in each animal and cortex when the animals were trained to discriminate sensory stimuli in the modality of the cortex being observed.

Because of the common carrier wave, each spatial pattern over its duration could be described by a 64×1 column vector and by a point in 64-space. Similar patterns formed clusters of points in 64-space, each with a center of gravity (centroid) corresponding to the time ensemble average spatial pattern for that cluster. Classes of patterns could be said to differ, if the distance between their centroids exceeded twice the standard deviation (2 SD radius) of two clusters. Membership of a given pattern in a class could be decided by calculating its Euclidean distance to a set of centroids and finding the smallest distance. This approach demonstrated that a minimum of 16 channels were necessary to discriminate between the neocortical AM patterns associated with two stimulus classes, CS+/CS−, that the rabbits had been trained to discriminate. However, the Euclidean distance yielded no information concerning the structures of clusters of points in 64-space, nor did it permit more than pairwise comparisons. Its greatest shortcoming was suspected with data sets that were not linearly separable. This could occur, for example, when a spherical cluster of points lies within another cluster of points distributed as an annulus. Both sets would have a similar centroid, thereby preventing classification by a distance measure.

The goal of this study was to apply the technique of Sammon (1969) for nonlinear mapping (NLM) to project clusters of points, representing AM patterns in 64-space, into a plane while preserving the distance relationships between the points. The results show that the discriminative power of a method for cross-classification using the two-dimensional points (after NLM) was similar to that afforded by the use of the complementary 64-dimensional points. This finding indicated that there was little to no structural distortion involved

in the NLM process. The power added by the NLM technique was the identification of stimulus-related structure not otherwise accessible to view in the high-dimensional data. The tradeoff is an increase in computational time to calculate the dimensional reduction.

2. Experimental methods

2.1. Animal preparation

New Zealand White (NZW) rabbits were chronically implanted with arrays of 64, stainless-steel, formvar-coated electrodes (8×8 , 0.25 mm diameter, 0.79 mm interelectrode distance) (Eastman, 1975) onto the epidural surface of the left visual, auditory, or somatic cortex (Barrie et al., 1996). One rabbit was implanted with four arrays of 16 electrodes (a multi-sensory implant) onto the epidural surfaces of the left visual, auditory, somatic (4×4 , 0.25 mm diameter, 0.79 mm interelectrode distance), and entorhinal cortices (2×8 , 0.25 mm diameter, 1.0 mm interelectrode distance). Reference and ground leads for monopolar recording were placed, respectively, adjacent to each array and over the right frontal sinus. The implantation of recording and reference electrodes was conducted under full surgical anesthesia (4% isoflurane–oxygen mixture). Each electrode array was placed in a rectangular trephination, and K-Y jelly was applied to the margins of the opening. Acrylic cement fixed the array to the skull, and reference wires (attached to screws in the skull) were wound around and cemented to the array stalk as rebar. All procedures were conducted according to a protocol approved by the University of California at Berkeley Animal Care and Use Committee and with veterinary supervision by the Office of Laboratory Animal Care. After the conclusion of all experiments, each animal was sacrificed by pentobarbital sodium overdose (120 mg/kg iv), and the site of implantation was dissected to check for cortical tissue damage, bone regrowth, proper array placement, or other post-mortem anomalies.

2.2. Experimental paradigm

After recovery from surgery, each rabbit was familiarized for 3 weeks to the recording environment by placing it into a restraining carrier, with skin clips for the delivery of the unconditioned stimulus (UCS) applied to the upper-left cheek, and a pneumograph belt to record the respiratory conditioned response (CR) from the chest. The restraining carrier was placed into an electrically shielded, dark box; white noise at 72 dB was used for masking. After familiarization, each rabbit was classically conditioned to discriminate between two similar stimuli in the same modality. Data were ac-

quired from 40 EEG trials consisting of 20 unreinforced stimuli (CS –) and 20 reinforced stimuli (CS +) delivered randomly in time and sequence, with exploratory sniffing (Davis and Freeman, 1982) as the CR. Every EEG record was 6 s. The CS –/CS + arrived at the rabbit after 3 s, and the UCS arrived at the cheek after 6 s. The UCS, consisting of four to five electrical pulses (1–5 mA) within a window of 10 ms, was aversive but not painful. The CS was a bright or dim full-field flash (3.6 vs. 2.8 footcandles (fc)); two amplitude-invariant sinusoidal tones (500 vs. 5000 Hz), delivered binaurally by earphones at 72–84 dB above the masking noise; or a puff of air to the right cheek or right hindquarters for the visual, auditory, or somatic preparations, respectively. This experimental paradigm was repeated twice.

EEGs recorded monopolarly were amplified and acquired with World Precision Instruments ISO 4/8 fixed-gain, differential amplifiers. The signal was filtered with single-pole, first-order analog RC filters (6 dB/octave fall-off) set at 100 Hz (3-dB point) and 0.1 Hz. Records of 64, 12-bit samples multiplexed at 10 μ s were recorded at 500 Hz. Data were stored onto magnetic media for later analysis. Bad signals caused by movement or other artifact were replaced by substitution with the average signals from two adjacent recording channels. There were no more than ten bad channels per experiment.

3. Data analysis

The EEG records from each experiment were edited for movement artifacts, 60 Hz contamination, and faulty connections. DC offsets from the amplifiers were removed by setting the EEG signal from each channel to zero mean in each 6-s trial. Spatial ensemble averages (SEA) and SDs of the recordings were made by averaging each of the 64-channels into one time series (Fig. 1a). Spectral analysis of the SEAs was accomplished by the fast Fourier transform (FFT) (Press et al., 1988) with Hanning to smooth the edge effects. Each spectral decomposition was averaged across trials to produce an ensemble average PSD and standard error (SE) to the 95% confidence level (Fig. 1b). Using the 20–100-Hz domain, a line was regressed onto the log average PSD vs. log frequency. A subsequent determination of excess spectral power (above the $1/f$ level), from both stimulus classes, was made by measuring where the lower 95% confidence interval of the standard error (SE) of the PSD was above the regression line (Barrie et al., 1996). Spectral segments of excess power were accumulated over trials and displayed as a density plot in time–frequency coordinates (Fig. 1c).

Two techniques for discriminating CS –/CS + AM spatial patterns within fixed temporal windows were compared. A technique for the nonlinear mapping of

64-dimensional spatial EEG patterns into two dimensions (Viana Di Prisco and Freeman, 1985) followed by cross-classification was contrasted with the cross-classification of the original patterns in 64-space (previously characterized by Barrie et al., 1996). In both cases the RMS amplitude was calculated for each of the 64 EEG traces using 128-ms windows stepped across each record of an experiment at 20-ms intervals. Use of the RMS to calculate the EEG spatial patterns was justified, because singular value decomposition (SVD) of the 64 EEG traces in 128-ms segments yielded > 90% of the variance in the first component. For each window (j), a 1×64 column vector ($\vec{V}^{(i,j)}$), representing the 64-dimensional RMS spatial pattern, was calculated using Eq. (1),

$$\vec{V}^{(i,j)} = \sqrt{\left(\sum_{k=1}^{\tilde{n}} A_k^2 - 1/\tilde{n} \cdot \left(\sum_{k=1}^{\tilde{n}} A_k \right)^2 \right) / (\tilde{n} - 1)} \quad \forall$$

$$k \in \{1, 2, \dots, 64\}, \quad i \in \{1, 2, \dots, q\}, \quad j \in \{1, 2, \dots, n\} \quad (1)$$

where \tilde{n} was the number of points within each window (64 points at a digitizing rate of 500 Hz represented a 128-ms window), k was the channel index, i was the record index, q was the number of records (40), n was the number of windows per record, A was the EEG amplitude in microvolts, and V was the RMS amplitude. Each 128-ms spatial frame was normalized to zero mean and unit SD to remove global amplitude differences, such as those imposed by stimuli of differing intensity and by varying levels of arousal and motivation (Freeman, 1975). The application of Eq. (1) to the EEG segments yielded a series of normalized, 64-dimensional spatial patterns.

For every experiment (40 trials) a series of n , 64-dimensional RMS spatial patterns was initially calculated. A method of nonlinear mapping (Sammon, 1969) was then used to test whether the CS – AM patterns could be separated from the CS + AM patterns, and whether projecting the 40, 64-dimensional vectors into two dimensions could characterize or capture properties of the original 40 vectors within a temporal epoch. The principle of mapping a group of points $\vec{V}^{(i,j)}$ from an a -dimensional space (64) to a group of points $\vec{W}^{(i,j)}$ in a two-dimensional projection plane was based on a minimizing procedure. For each window (j), q 64-dimensional points were mapped to a two-dimensional plane initially defined by the largest two coordinate axes of variance. An a priori energy (E) was calculated on inter-distant points using Eq. (2),

$$E(d_{f,g}) = \sum_{1=f < g = q} (d_{f,g}^* - d_{f,g})^2 / d_{f,g}^* / \sum_{1=f < g = q} d_{f,g}^* \quad (2)$$

where $d_{f,g}$ was the distance between the points $\vec{V}^{(f,j)}$ and $\vec{V}^{(g,j)}$ in 64-dimensional space and $d_{f,g}^*$ was the distance between the points $\vec{W}^{(f,j)}$ and $\vec{W}^{(g,j)}$ on the

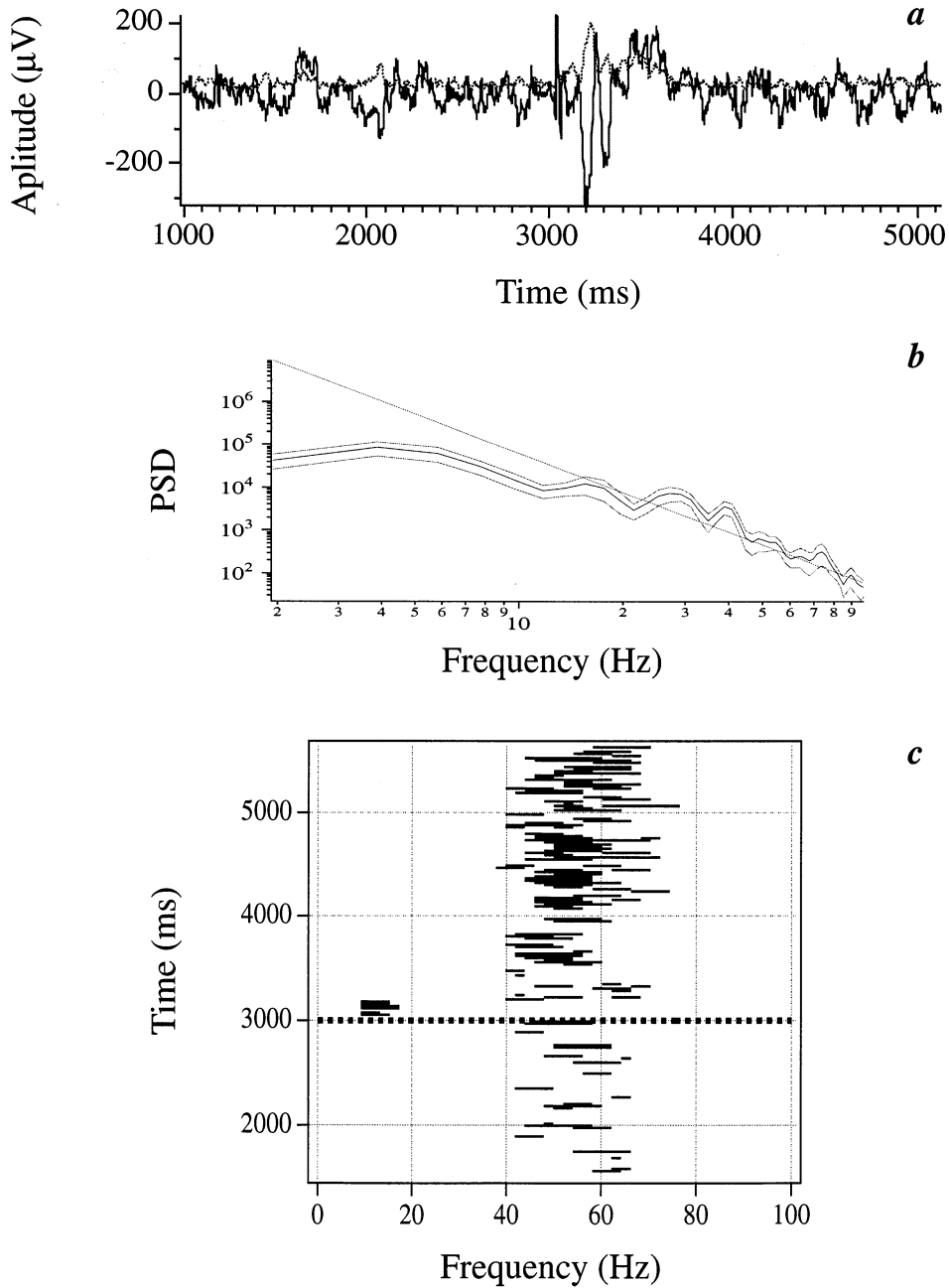


Fig. 1. (a) Spatial ensemble average (solid trace) and standard deviation (SD, dashed trace) of the EEGs simultaneously recorded from 64 electrodes on the visual cortex during a single representative trial. The low SD reflected the common waveform across the spatial array. (b) Temporal spectral analysis. The average PSD (solid curve) and 95% standard error (dashed curve) were calculated from 40, 128-ms records from a visual cortical experiment using both stimulus classes. A line (solid line) was subsequently regressed onto the 20–100-Hz domain of the average PSD in log–log coordinates. (c) Spectral segments where the 95% SE of the PSD (lower bounds), from a somatosensory experiment, exceeded the regression line were marked. A graph of those segments illustrated that the γ -band power of the somatic EEG rose after the arrival of the CS. This finding was similar for the visual and auditory EEG.

plane. By rotating the two-dimensional plane to preserve the distances between points while optimizing the separation into clusters, E was allowed to evolve for t iterations until a desired rate of stabilization (ε) was observed using a gradient descent algorithm,

$$|\vec{M}_{t+1} - \vec{M}_t| < \varepsilon, \quad (3)$$

where \vec{M} was the vector $\vec{V}^{(i,j)} \quad \forall \quad i \in \{1, 2, \dots, q\}$ for q records within one temporal window. The evolution of the points followed Eq. (4),

$$\vec{M}_{t+1} = \vec{M}_t + h \text{grad } E / |\Delta E| \quad (4)$$

where ΔE was the Hessian matrix, or second derivative, of E with respect to $d_{f,g}$ and h was the parameter

for the speed of convergence, $h = 0.3$ (Sammon, 1969). Points mapped onto the plane were then normalized for each temporal epoch.

Cross-classification was used as a benchmark to test whether or not the CS – RMS spatial patterns within each temporal epoch could be separated from the CS + patterns within that same epoch. Briefly, for any window (j) the 20 CS – patterns were separated into two subgroups ($m = 1, 3$) and the 20 CS + patterns were separated into another two subgroups ($m = 2, 4$); each subgroup (m) consisted of alternating patterns sampled evenly across the set of 20 patterns. The vectors within groups 1 and 2 were averaged to find centroids (C) 1 and 2. The Euclidean distance (D), in either 64- or 2-space (for the nonlinearly mapped patterns), was calculated between all of the vectors within subgroups 3, 4 to the centroids 1, 2 using Eq. (5),

$$D(\vec{C}^{(m,j)}, \vec{R}^{(i,j)}) = \sqrt{\sum_{k=1}^{\tilde{d}} (C_k^{(m,j)} - R_k^{(i,j)})^2} \quad \forall \tilde{d} = 1, 2, \dots, 64 \quad \text{or} \quad \tilde{d} = 1, 2 \quad (5)$$

where $\vec{R} = \vec{V}$ for the 64-dimensional patterns, $\vec{R} = \vec{W}$ for the two-dimensional (NLM) patterns, and \tilde{d} was the dimension count. If the distance from any vector to its respective centroid was less than the distance to the opposite centroid (as defined in Eq. (6)), then that vector was said to classify correctly,

$$D(\vec{C}^{(2\tilde{m}-1,j)}, \vec{R}^{(i,j)}) < D(\vec{C}^{(2\tilde{m},j)}, \vec{R}^{(i,j)}) \quad \forall \tilde{m} \in \{1, 2\}, \quad i \in \{20(2 - \tilde{m}) + 1, \dots, 20(3 - \tilde{m})\} \quad (6)$$

where $\tilde{m} = 1$ represents centroids 1, 2 and indexes i to patterns 21–40; and where $\tilde{m} = 2$ represents centroids 3, 4 and indexes i to patterns 1–20. This process was cross-validated by using the patterns in subgroups 3, 4 to classify the patterns in subgroups 1,2. The result was a temporal sequence of ratios ($x:40$), where x was the number of correctly classifying patterns for each window. These ratios were converted into a time series of probability values, whether a particular x value could have occurred by chance, by calculating a binomial probability distribution (based on a sample size of 40).

4. Results

Prior findings in EEGs from arrays on neocortices were as follows: (a) the EEGs had aperiodic oscillations with no apparent temporal structure indicating post-stimulus information processing other than the typical evoked potential (Fig. 1a). (b) Simultaneous recording at multiple sites gave a common wave form, which comprised $>90\%$ of the variance under SVD, and which was most easily observed by spatial ensemble averaging over single trials (Fig. 1a, solid curve) and documented by the low standard deviation (Fig. 1a,

dashed curve). (c) The power spectrum in log–log coordinates showed a nearly linear relationship between decreasing power and increasing frequency (Fig. 1b). (d) The common wave form revealed spatial patterns of amplitude modulation (AM) in brief time segments, that were extracted by the dominant spatial mode in SVD, by the gain coefficients of the FFT of the 64 traces at the dominant frequencies, or most simply by the 64 root mean square (RMS, Eq. (1)) values of the 64 EEG segments. (e) These AM patterns recurred in classifiable shapes following training to discriminate between CS + and CS – average patterns – or centroids (Fig. 2a, c), although no patterns were identical but varied around the means (SDs in Fig. 2b, d). (f) The AM patterns were best classified after bandpass filtering the EEGs in the γ range (20–80 Hz in rabbits). Review of the PSD spectra showed that an excess of power above the regression line to the PSD curve occurred in the γ range particularly in the poststimulus period as compared with the prestimulus period (Fig. 1c). (g) The EEG information supporting AM pattern classification was uniformly distributed over the arrays, no channel being any more or less important than any other. The goodness of classification (i.e. the probability that the levels of pattern discrimination observed were below the 99% significance level, $P < 0.01$) was proportional to the number of channels used. (h) Separation of CS + /CS – segments occurred in brief time periods lasting on the order of 100 ms, starting just after CS arrival and recurring at irregular time intervals between the CS and CR, reflecting the endogenous determination of the exact times of onset of the classifiable AM patterns.

Inspection of Fig. 2 shows the difficulty of judging whether any two AM patterns or classes of AM patterns differ significantly. EEG traces are equally important from channels with both high and low mean amplitudes and both high and low SDs. The heuristic value of projecting the clusters of AM patterns into a plane by use of NLM (Eqs. (2)–(4)) is immediately apparent in Fig. 3. Sets of 40 AM patterns are expressed as points in 64-space projected into two-space. Fig. 3a shows the locations in a representative segment from the control period. The globular shape of the global cluster reflects the normal distribution of each of the 64 RMS values, and the intermingling of the open circles (CS +) and solid box (CS –) reflects the lack of difference of the AM patterns during the intertrial intervals. The separation of AM patterns is seen in Fig. 3b just after the arrival of the CS + or CS –. A second separation occurs about 300 ms later (Fig. 3c), and a third typically several hundred ms later (Fig. 3d), though less clearly or convincingly, owing at least in part to the failure of these endogenous events to recur in the same poststimulus time intervals on successive trials. In Fig. 3d the typically tighter clustering of the

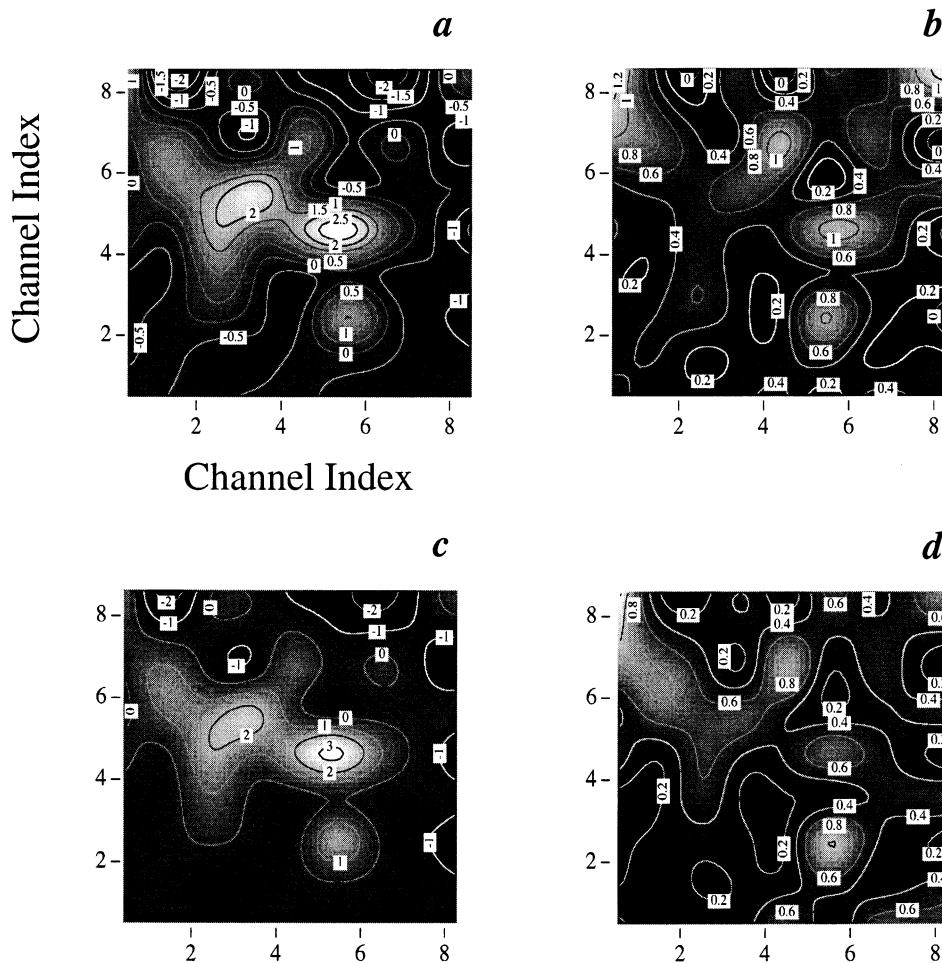


Fig. 2. These figures illustrate the CS + and CS – mean patterns (or centroids), and their associated (SD), calculated for the CS + and CS – stimulus classes by averaging the RMS of the EEG from 20 records for one, 128-ms prestimulus temporal epoch spanning 2200–2328 ms. This epoch was extracted from the control period of a somatic experiment. (a) CS – centroid; (b) SD associated with the centroid from (a); (c) CS + centroid; (d) SD associated with the centroid from (c). The probability that the 64-dimensional CS –/CS + spatial patterns are different is a function of the distance between the centroids in units of SD in the time domain; this cannot be determined by visualizing the individual 64-dimensional patterns. Contours in (a) and (c) represent mean RMS amplitude values normalized to zero mean and unit SD (gray scale from white to black represents high to low values).

CS + AM patterns (lower SD) compared with that of the CS – AM patterns (higher SD) offers an opportunity to separate the clusters by applying the modified Grassberger–Procaccia (Grassberger and Procaccia, 1983) algorithm to evaluate c_2 and its statistical significance (see below).

Nonlinear mapping served to show that the AM patterns just after arrival of the CSs differed not only from each other between trials but also from the preceding AM patterns in the control period in the same trials. Fig. 4a, c shows the overlapping clusters of points from two representative times in the control period (circle at 2200 ms, box at 2600 ms) for CS – (a) and CS + (c) trials, whereas Fig. 4b, d shows the distinct separation of the cluster from one of the two times in the control period (circle at 2200 ms) versus the cluster of AM patterns after stimulus arrival (box at 3200 ms). NLM also revealed the differences in AM

patterns at successive time periods after CS arrival, as shown in Fig. 5b where the clusters of points labeled ‘1’, ‘2’ and ‘3’ demarcate the AM patterns at three successive times between the CS and CR. Separations of AM patterns with respect to CSs did not occur in the control period (Fig. 5a). Finally, the projection by NLM from 16- into two-space served to display clusters of the AM patterns in EEGs simultaneously from four cortices (visual, auditory, somatic, and entorhinal) in a subject with multiple 4×4 arrays in one subject (Fig. 5c). As predicted from visual inspection of contour plots, each cortex had a unique AM pattern, but with incomplete separation of clusters principally owing to outliers.

Previous work documented multiple poststimulus epochs where the 64-dimensional CS-spatial patterns could be partially but significantly separated from the CS + patterns (Barrie et al., 1996) by stepping a fixed-

length window across 40 records of EEG data at a fixed interval and applying a method of cross-classification to the individual RMS patterns. That finding was replicated here by stepping a 128-ms window at 20-ms intervals across 40 records of EEG data (20 CS – and 20 CS +) and calculating the 64 RMS values. The AM patterns were separated into their respective stimulus classes with the Euclidean distance metric in 64-space. Those findings were supported and extended by nonlinear mapping the same 64-dimensional AM patterns onto a plane. The Euclidean distance metric and subsequent cross-validation was then repeated in two-space. When an endogenously generated event occurred in sensory neocortex, the levels of significant CS – /CS + pattern discrimination ($P < 0.01$) increased for both the 64- and two-dimensional classification analysis. Using the Spearman rank-order nonparametric correlation coefficient (Press et al., 1988), the values from both discriminative methods were significantly correlated ($P < 0.01$). This correlation demonstrated that re-mapping the EEG to two coordinates preserved the relative distance relations of the 64-dimensional structure.

5. Discussion

The recent emergence and rapid development of techniques for brain imaging using EEG, MEG, optical dyes,

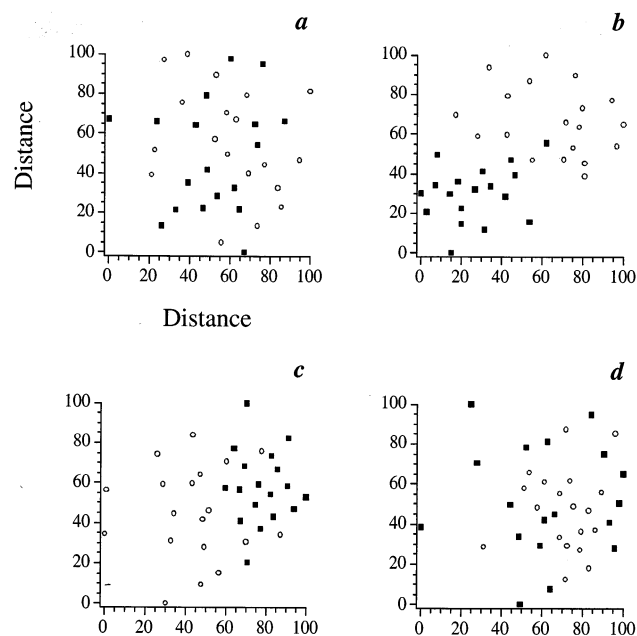


Fig. 3. Nonlinear mapping of the visual cortical EEG. Each point represents an EEG spatial RMS amplitude pattern remapped from 64-space onto a plane. The open circles indicate CS + stimuli and the filled boxes indicate CS – stimuli. (a) Prestimulus EEG, 2000–2128-ms prestimulus mixing; (b) stimulus arrival, 3000–3128-ms global separation; (c) poststimulus EEG, 3300–3428-ms global separation; (d) late poststimulus EEG, 4050–4178-ms intermediate mixing.

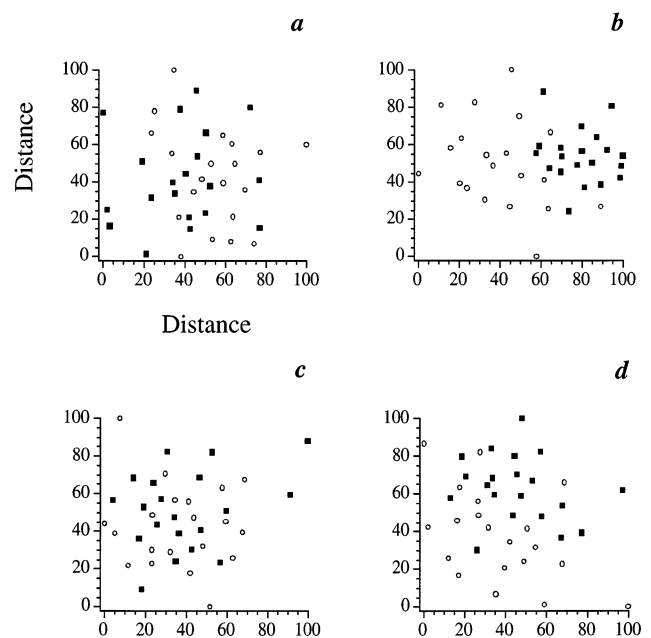


Fig. 4. Generation of novel spatial EEG amplitude patterns from the visual cortex. Pre- and poststimulus 64-dimensional EEG spatial patterns from one stimulus type (either CS + or CS –) were nonlinearly mapped to two dimensions. The left column (a, CS –; c, CS +) illustrates two temporal epochs of prestimulus patterns projected onto a plane (circle, 2200 ms; box, 2600 ms). The right column (b, CS –; d, CS +) illustrates prestimulus and poststimulus patterns projected onto a plane (circle, 2200 ms; box, 3200 ms). These results illustrate that the EEG patterns formed during a poststimulus temporal epoch, from both stimulus classes, are significantly different from the prestimulus patterns. The prestimulus patterns do not have a regular structure that allows such discrimination.

blood flow, and metabolic labeling offer opportunities for new insights into brain functioning that cannot be obtained from measurements only of time series. The results of spatial mapping offer compelling vistas when they are presented as contour plots in full color, showing patterns of brain activity that are obviously different on visual inspection. However, judgements of the reliability of such vistas must be based on multiple replications, and it is difficult for human observers to retain in view a sufficient number of examples to assess them properly. Although the variance of spatial patterns can be reduced by time ensemble averaging, the sample means may lose crucial features through smoothing and will require replication in their turn to establish reliability. There are diminishing returns in grand averages of averages over trials and subjects. Color contour plots have their greatest value when the features to be distinguished are localized within frames, as when attempts are made to localize sensory-evoked unit activity, epileptic foci, or sites of cognitive functions in cerebral cortex. They are least useful in distinguishing distributed information in the form of interference patterns, where peaks and valleys are equally important. The AM patterns from primary sensory cortical EEGs are of this kind.

A variety of multivariate statistical methods is available for collecting and evaluating sets of spatial images of all kinds, which have been digitized and expressed as high-dimensional vectors. The methods include stepwise discriminant analysis, factor analysis, regressive trees (CART; Grajski and Freeman, 1989), and digital image classification (Rosenfeld and Kak, 1976). In the authors' experience with EEG AM patterns the simplest and most effective approach to exploration of large data sets has been to express each AM pattern as a point in 64-space, to locate classes of AM patterns by calculating centers of gravity of clusters, and to define membership of single events in classes by the Euclidean distance metric. The main

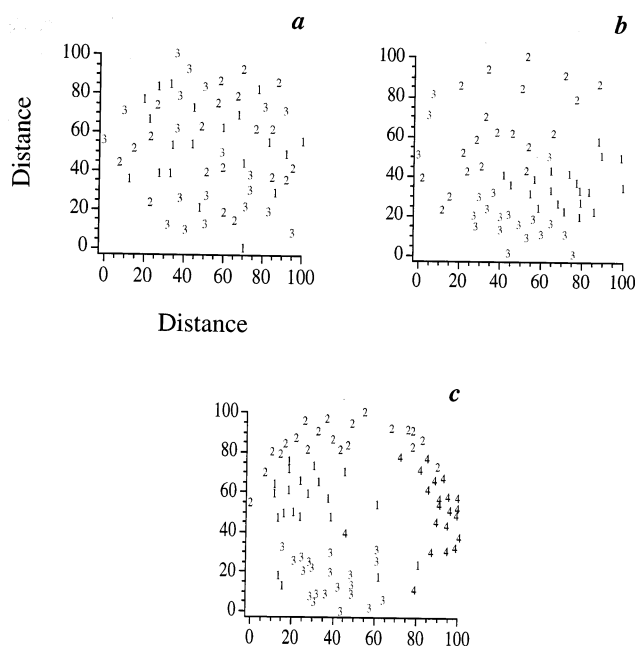


Fig. 5. Nonlinear mapping of temporally distinct EEG windows. The EEG from 20 CS + visual cortical records was temporally bandpass filtered, converted into 64-dimensional RMS vectors from three, 120-ms windows separated by 500-ms intervals, and remapped onto a plane. (a) Prestimulus EEG: (1) 1000–1120 ms; (2) 1500–1620 ms; and (3) 2000–2120 ms. (b) Poststimulus EEG: (1) 3000–3120 ms; (2) 3500–3620 ms; and (3) 4000–4120 ms. The segments in (b) were chosen because they corresponded to the temporal epochs where the CS + /CS – EEG patterns could be separated for this experiment. The EEG patterns within each of the different poststimulus epochs formed distinct clusters on the plane indicating that three distinct classes of EEG patterns were generated in response to one stimulus class. No such observation was made in the prestimulus data. (c) Nonlinear mapping from a multi-sensory EEG recording. Four classes of EEG were projected from 16 dimensions onto a plane. The EEG from this experiment was simultaneously recorded from arrays of electrodes implanted onto the epidural surfaces of the somatic, auditory, visual, and entorhinal cortices and temporally bandpass filtered between 20 and 80 Hz. (1) Somatic, (2) auditory, (3) visual, and (4) entorhinal EEG. Each point within a group (i.e. 1–4) represents one of 21, 128-ms records of data. The EEGs recorded from four different cortical areas cluster into four distinct groups on the plane.

shortcomings of this approach have been the restriction to pair-wise comparisons between classes, the lack of a means to visualize the shapes of the cluster distributions, and the insensitivity to distinctive clusters that are not linearly separable, such that a hyper-plane can be passed between them.

The NLM algorithm projects the high-dimensional clusters onto a plane without losing the internal structure of the distributions. This was shown by comparing the measures of goodness of pattern discrimination before and after projection from a hyper-space and finding nearly identical results in the time series of classification values from the two analyses. The demonstration of linear separability then becomes a matter of drawing a line between the differing clusters. The globular shapes of distributions of the total data sets, particularly from controls where there is no separation, reflects the normality of the distributions of AM points based in the Gaussian distributions of the RMS values; it gives access to outliers, which can be seriously detrimental to Euclidean classification by distorting the locations of centroids.

6. Variables used

| | |
|---------------|--|
| <i>A</i> | EEG signal |
| <i>a</i> | 64-dimensional space |
| <i>b</i> | arrival space (a plane) |
| <i>c</i> | centroid |
| <i>d</i> | distance in 64-space |
| <i>d*</i> | distance in two-space |
| \tilde{d} | dimension count |
| <i>D</i> | Euclidean distance |
| <i>E</i> | energy |
| ΔE | second derivative of <i>E</i> |
| ε | rate of stabilization |
| <i>f</i> | record index 1 |
| <i>g</i> | record index 2 |
| <i>h</i> | speed of convergence parameter |
| <i>i</i> | record index |
| <i>j</i> | temporal window index |
| <i>k</i> | channel index |
| <i>m</i> | subgroup index |
| \vec{M} | the vector $\vec{V}^{(i,j)} \quad \forall i \in \{1,2,\dots,q\}$ for <i>q</i> records within one |
| <i>n</i> | number of temporal windows |
| \tilde{n} | number of EEG points/temporal window |
| <i>q</i> | total number of records |
| <i>R</i> | EEG asterisk (refers to either 64- or two-dimensional point) |
| <i>t</i> | time |
| \vec{V} | RMS amplitude vector in 64-space |
| \vec{W} | RMS amplitude vector in two-space |
| <i>x</i> | number of correctly classifying records |

Acknowledgements

The authors wish to thank M.D. Lenhart for his invaluable assistance with the experimental preparation and P. German, A. Smart, G. Gaal for assistance with the multi-sensory preparation. D. Holcman would like to thank W.J. Freeman for the invitation to work in his lab during the summer of 1996 and Natalie Rouach for remarks on the manuscript. More information on the background and research interests of the authors may be obtained on the Freeman Lab WWW site by accessing: <http://sulcus.berkeley.edu> on the Internet. This work was supported by a grant from the National Institute of Mental Health, MH06686.

References

- Barrie JM, Freeman WJ, Lenhart MD. Spatiotemporal analysis of prepyriform, visual, auditory, and somesthetic surface EEGs in trained rabbits. *J Neurophysiol* 1996;76:520–39.
- Davis GW, Freeman WJ. On-line detection of respiratory events applied to behavioral conditioning in rabbits. *IEEE Trans Biomed Eng* 1982;29:453–6.
- DeMott DW. *Toposcopic Studies of Learning*. Springfield, IL: Thomas, 1970.
- Eastman C. Construction of miniature electrode arrays for recording cortical surface potentials. *J Electrophysiol Tech* 1975;5:28–30.
- Freeman WJ. *Mass Action in the Nervous System*. New York: Academic Press, 1975.
- Freeman WJ, Viana Di Prisco G. Relation of olfactory EEG to behavior: time series analysis. *Behav Neurosci* 1986;100:753–63.
- Grajski KA, Freeman WJ. Spatial EEG correlates of nonassociative and associative olfactory learning in rabbits. *Behav Neurosci* 1989;103:790–804.
- Grassberger P, Procaccia I. Measuring the strangeness of strange attractors. *Physica D* 1983;9:189–205.
- Lilly JC, Cherry RB. Surface movements of click responses from acoustic cerebral cortex of cat: leading and trailing edges of a response figure. *J Neurophysiol* 1954;17:521–32.
- Press WH, Flannery BP, Teukolsky SA, Vetterling WT. *Numerical Recipes in C*. Cambridge, UK: Cambridge University Press, 1988.
- Rosenfeld A, Kak AC. *Digital Picture Processing*. New York: Academic Press, 1976.
- Sammon JW. A nonlinear mapping for data structure analysis. *IEEE Trans Comput* 1969;C-18:401–9.
- Viana Di Prisco G, Freeman WJ. Odor-related bulbar EEG spatial pattern analysis during appetitive conditioning in rabbits. *Behav Neurosci* 1985;99:964–78.